Extended x-ray-absorption fine structure above the Co $L_{2,3}$ edges in ion-beam-synthesized $CoSi_2$

S. Eisebitt, J.-E. Rubensson, T. Böske, and W. Eberhardt
Institut für Festkörperforschung, Forschungszentrum Jülich, D-52425 Jülich, Germany
(Received 18 June 1993; revised manuscript received 17 August 1993)

An analysis of the extended x-ray-absorption fine structure recorded at the Co $L_{2,3}$ edges of $CoSi_2$ is presented. Absorption was monitored by partial fluorescence yield, allowing us to investigate samples buried in a silicon wafer by means of ion-beam synthesis. The absorption spectrum is not distorted by Bragg diffraction beams due to the low photon energies. The additional Co L_1 background is modeled by a splining procedure. The first-shell Co-Si distance in the annealed specimen was determined to be 2.32 ± 0.05 Å.

I. INTRODUCTION

In the past decade $CoSi_2$ has attracted much interest because it can be grown epitaxially on Si due to the small lattice mismatch. The low specific resistivity of $CoSi_2$ makes it suitable for special microelectronic devices such as metal-base (MBT) and permeable-base (PBT) transistors.[1–4] Ion-beam synthesis (IBS) has overcome problems associated with the epitaxial growth of $CoSi_2$ on Si(100) encountered by conventional deposition techniques.[5] With IBS, buried layers of $CoSi_2$ and other transition-metal (TM) silicides with sharp interfaces to a Si substrate can be formed.

Studies of the extended x-ray-absorption fine structure (EXAFS) at absorption edges of TM atoms can be used to investigate the local geometry in these silicides *in situ*. In devices such as the MBT or PBT, the silicide is buried in a Si wafer and covered by a Si cap layer which is typically thicker than 200 Å. This geometry makes it impossible to detect the x-ray absorption in the transmission mode or by electron yield detection. It is nevertheless possible to detect the EXAFS by monitoring the fluorescence yield (FY) due to the larger penetration depth of photons.[6–8]

As intense Bragg diffraction beams are generated in the crystalline Si environment, it is difficult to combine conventional EXAFS spectroscopy at the Co K edge (Co K EXAFS) with the FY detection mode needed to investigate buried structures. During the EXAFS photon energy scan the Bragg beams move and produce huge peaks in the absorption spectrum when hitting the detector. Thus, either these distortions have to be removed from the data (if possible) or a special setup has to be used to selectively block the Bragg beams in front of the detector.[9]

In contrast, this is no problem if the EXAFS of the Co $L_{2,3}$ edge (Co L EXAFS) is investigated, since no Bragg diffraction peaks are present due to the lower photon energies. Consequently, the absence of Bragg diffraction peaks makes L EXAFS favorable for samples buried in crystalline material such as a Si wafer. Nevertheless, certain difficulties in the data analysis arise due to the superposition of absorption features related to the Co L_3, L_2, and L_1 edges. Because of these complications, EXAFS investigations at the Co L edges in particular and the $3d$ TM L edges in general have been rare in the past.[10,11]

In this paper we present an analysis of the EXAFS recorded at the Co L edges by means of FY detection in order to discuss the advantages and limitations of this technique for the investigation of buried $3d$ TM structures.

II. EXPERIMENT

We have chosen a $CoSi_2$ layer buried in a Si(100) wafer[12] for this investigation. Pure $CoSi_2$ crystallizes in the cubic CaF_2 structure with a unit cell edge length of 5.365 Å.[13] From the viewpoint of a Co central atom, this results in 8 first shell Si neighbors at a distance of 2.323 Å and 12 second shell Co neighbors at a distance of 3.794 Å.

Samples were prepared by 100 keV Co ion implantation into a Si(111) wafer at a temperature of 375 °C.[12] The implantation dose was 1.4×10^{17} atoms/cm^2. The samples were annealed at 600 °C for 1 h followed by 1000 °C for 30 min after the implantation process.

The annealed specimens consist of a single crystalline, stoichiometric $CoSi_2$ layer of 500 Å thickness with sharp interfaces buried under a 270 Å Si cap layer, as verified by Rutherford backscattering spectroscopy, electron microscopy studies,[12] optical studies,[14] and investigations of the electronic structure.[15]

The FY-EXAFS spectra were measured at the HE-PGM2 monochromator[16] at Berliner Elektronenspeicherring Gesellschaft für Synchrotronstrahlung GmbH (BESSY). The monochromator resolution was estimated to be 2 eV at the Co L_3 edge. Using a Ge detector that allowed us to monitor the Co L emission with a resolution of about 100 eV, the absorption spectra were recorded in a partial fluorescence yield mode.

III. RESULTS AND DISCUSSION

Figure 1 shows an EXAFS spectrum of a $CoSi_2$ layer buried in a (100)Si wafer recorded by FY detection. As

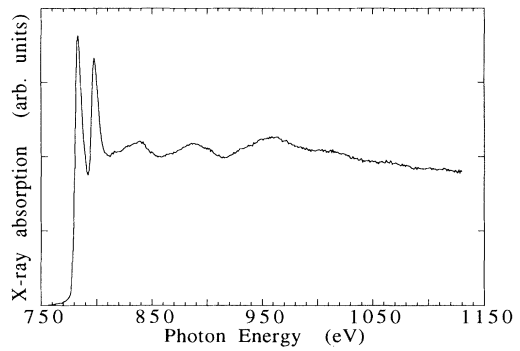

FIG. 1. An overview of the Co L EXAFS spectrum as recorded by partial fluorescence yield detection. The first 40 eV of the spectrum are dominated by the Co $L_{2,3}$ near edge structures. In the energy region above, EXAFS oscillations are visible. No distorting peaks due to Bragg diffraction beams are present.

expected, no Bragg diffraction peaks distort the spectrum. Above the Co L_3 and L_2 x-ray-absorption near edge structures seen in Fig. 1, strong EXAFS oscillations are clearly visible up to the end of the spectrum. The onset of an additional absorption stucture is expected to occur at a photon energy of about 925 eV (Ref. 17) due to opening of the Co L_1 absorption channel.

With respect to EXAFS data analysis, the spectrum can be divided into three distinct regions as indicated in Fig. 2: Region I is characterized by the superposition of EXAFS associated with the Co L_3 and L_2 absorption edges. In region II the Co L_1 near edge structure is additionally present. The photoabsorption cross section for the Co $2s$ electrons just above the $2s$ threshold is about 15% of the cross section for the Co $2p$ electrons.[18,19] Thus the near edge structure produced by the $2s$ electrons is of about the same magnitude as the $L_{2,3}$ EXAFS wiggles due to the $2p$ electrons, whose amplitudes are about 5%

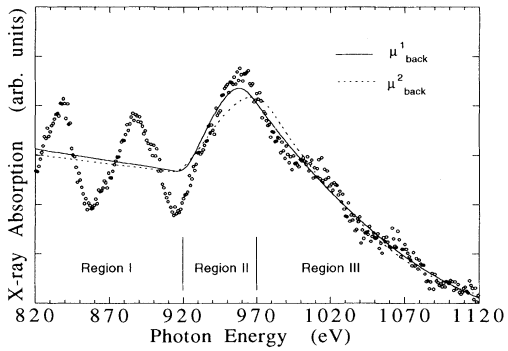

FIG. 2. The EXAFS region of the spectrum presented in Fig. 1 is shown in detail. In region II the absorption rises in addition to the EXAFS oscillations due to the onset of the Co L_1 absorption. The near edge structure of the Co L_1 absorption produces an additional background with respect to the Co L EXAFS analysis. Two different polysplines $\mu^{1,2}_{\text{back}}$ modeling the background are shown.

of the $L_{2,3}$ edge jump in $CoSi_2$. Though the Co L_1 near edge structure cannot at first sight be distinguished from the $L_{2,3}$ EXAFS structures, its presence is confirmed by the overall rise of the absorption coefficient in this energy range and the changed background slope in the energy range above. In region III, the main features are again the EXAFS oscillations connected to the $L_{2,3}$ edges. As mentioned before, the background slope differs from region I due to the presence of the L_1 absorption channel. The L_1 EXAFS present in this photon energy range is negligible compared to the $L_{2,3}$ EXAFS on behalf of the different cross sections.

As is obvious from Fig. 2, the impact of the additional Co L_1 absorption in region II is much larger with respect to EXAFS data analysis than the superposition of the L_3 and L_2 EXAFS. This is due to the fact that the EXAFS generated by Co $2p_{3/2}$ and $2p_{1/2}$ electrons are to a first approximation characterized by the same frequencies since they are due to the same geometric structure. This approximation neglects the different kinetic energies of the scattered electrons due to the 15.2 eV spin-orbit splitting in Co. In this simple model, the superimposed $L_{2,3}$ EXAFS can be constructed from the L_3 EXAFS alone by superimposing the same spectrum shifted by 15.2 eV after scaling its intensity with a factor of 0.5 in order to take care of the different degeneracies of the $2p$ core levels.

We have performed model calculations for $CoSi_2$ to check the influence of the $L_{2,3}$ superposition on the determined distances and coordination numbers in this model. The superimposed $L_{2,3}$ EXAFS was calculated and analyzed as if it were generated by the L_3 edge only. Since E_0, the energy corresponding to zero wave vector in k space, is not clearly defined due to the contribution of the electrons of different core levels, it was handled as a free parameter in the EXAFS fitting analysis.

Since the spin-orbit splitting of 15 eV is small compared to the typical EXAFS oscillation period of about 60 eV in $CoSi_2$, the effect of this superposition is small with respect to the determination of interatomic distances, though it has some impact upon the EXAFS amplitude and hence the determination of coordination numbers. The errors induced to the determination of the first and second shell distances were found to be around 0.015 Å. Coordination numbers determined were not reliable using this simple model. They turned out to be about 50% too low for the second shell, which is more influenced than the first shell.

We therefore neglect the $L_{2,3}$ superposition in the following and treat the $L_{2,3}$ EXAFS as if it were generated by one L edge only and we will focus upon the determination of interatomic distances.

In contrast to the effect of $L_{2,3}$ superposition, the superposition of the L_1 near edge absorption structure in region II has a large effect upon the interpretation of the data in terms of the geometric structure. This is due to the fact that the near edge structure is dominated by electronic effects. Thus from the point of view of EXAFS analysis, the L_1 absorption appears as an additional background which is of the same magnitude as the $L_{2,3}$ EXAFS signal to be analyzed.

It is important to find a technique in order to account for this additional L_1 background. It would of course be most favorable to know the shape and magnitude of the Co L_1 near edge absorption structure (without the superposition of the $L_{2,3}$ EXAFS). To our knowledge, these data are presently not available. Due to this fact, we have chosen to model this additional L_1 background.

A set of cubic splines has been used to account for the smooth background $\mu_0(E)$ produced by the atomic absorption in EXAFS measurements.[20] For this purpose, the EXAFS spectrum is divided into equidistant intervals. On each interval, a cubic spline interpolation is performed under the condition that the splines have to match at the interval boundaries. In the following we will call the resulting function a "polyspline." Choosing the length of the intervals appropriately, this cubic polyspline is too "stiff" to follow the individual EXAFS oscillations, but they will follow the mean trend of the data. By means of this procedure the atomic background $\mu_0(k)$, where k denotes the electron wave vector, is modeled by the polyspline and can be used to determine $\chi(k) = [\mu(k) - \mu_0(k)]/\mu_0(k)$ from the recorded absorption data $\mu(E)$.

We use a similar polysplining technique to account for the additional background due to the Co L_1 edge. If the order of the spline polynomial is increased, it will become less stiff and thus be able to follow the spectral features more closely. In order to use this procedure to model the additional L_1 background, the spline intervals have to be chosen properly. The aim is to "soften" the polyspline only in the region where the L_1 absorption is expected.

As the shape of the spline can be influenced to a large extent, it is important to have criteria judging the quality of the spline approximation. For this purpose the resulting Fourier transform can be used to judge the quality of the spline used. Strong peaks in the transform at distances around 1 Å reflect no physical property of the $CoSi_2$ system. Their appearance is thus an indication of poor polysplining. A second criterion is the shape of the first shell peak in the Fourier transform. Since this first shell is well separated from the second shell in $CoSi_2$, the corresponding peak in the Fourier transform should be symmetric with respect to the peak position.

Two polysplines satisfying this condition are shown in Fig. 2. They differ slightly in regions I and III, but the main difference is the L_1 edge modeled in region II. Using the polyspline backgrounds $\mu^1_{\text{back}}(E)$ (solid line) and $\mu^2_{\text{back}}(E)$ (dashed line) shown in Fig. 2 to account for the (atomic and L_1) background in the EXAFS data, $\chi(k) = [\mu(k) - \mu_{\text{back}}(k)]/\mu_{\text{back}}(k)$ was calculated.

The corresponding Fourier transforms (FT's) are shown in Figs. 3(a) and 3(b). In both transforms a distinct first shell peak is visible. The corresponding Co-Si distance was determined by a fitting procedure to $k\chi(k)$ as 2.317 ± 0.007 Å using μ^1_{back} and as 2.312 ± 0.007 Å using μ^2_{back}. Errors denote the error of the fitting procedure only. The difference of 0.005 Å in the distances determined using the different polysplines gives an estimate for the error induced by the polysplining procedure as both splines were varied (within the constraints of the polysplining technique) as much as possible while still meeting the criteria discussed above. We estimate the overall error to be 0.05 Å. Thus we determine the Co-Si first neighbor distance in the IBS sample as 2.32 ± 0.05 Å. This distance agrees very well with the Co-Si distance literature value of 2.323 Å.[13] This agreement proves the validity of the Co L EXAFS analysis technique as the sample has been shown to consist of single crystalline $CoSi_2$ before.

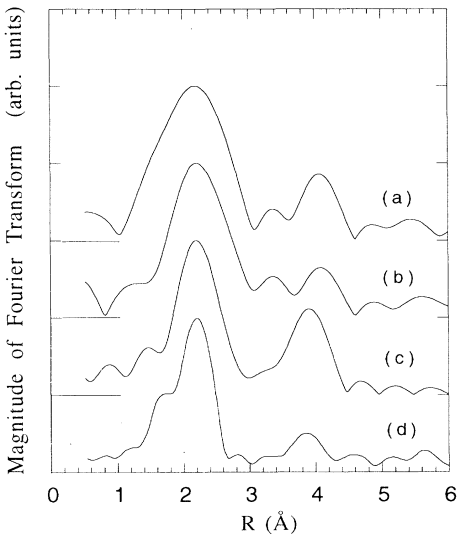

FIG. 3. In (a) and (b) we present the Fourier transforms of the data shown in Figs. 1 and 2. In (a) μ^1_{back} was used for background subtraction, while μ^2_{back} was used in (b) (see Fig. 2). In (c) the transform of a simulated Co L EXAFS spectrum using literature values for $CoSi_2$ is shown ($R_1 = 2.323$ Å, $R_2 = 3.794$ Å). For (a)–(c) the wave vector range covered is 6 $Å^{-1}$ and k^1 weighting was applied to $\chi(k)$ before the Fourier transformation. In (d) a FT obtained by Tan *et al.* (Ref. 9) using Co K EXAFS on a similar IBS sample is shown. Here, the wave vector range covered is 11 $Å^{-1}$. The spectrum was aligned on the first shell peak with (c) to account for different phase shift correction.

For comparison, the FT of a simulated Co L EXAFS spectrum including a Co-Si first shell distance of 2.323 Å and a second shell distance of 3.794 Å is shown in Fig. 3(c). As expected from the result of the fitting analysis, the first shell peaks of both experimental spectra agree in position with the theory shown in (c), although especially the first shell peak in (a) is considerably broadened. In contrast to the unambiguous identification of the first shell peaks in the experimental spectra, no clear second shell peak as seen in the simulation can be identified.

In Fig. 3(d) data recently presented by Tan *et al.*[9,21] obtained by Co K EXAFS of a similar IBS sample is shown for comparison. Since different k weighting prior to the Fourier transformation and different phase shift corrections were used, the comparison of the FT's can only be qualitative. To roughly account for the latter difference, the FT presented by Tan *et al.* was shifted on the r axis to align the first shell peak with the calculated FT in (c).

As in the L EXAFS spectra, the dominant feature in the K EXAFS FT is the first shell peak. The smaller full width at half maximum of this peak compared to the corresponding peak in the L EXAFS FT's is mainly due to the larger wave vector range of 11 $Å^{-1}$ covered in the K EXAFS experiment in contrast to 6 $Å^{-1}$ for our L EXAFS experiment. As seen from comparison of Figs. 3(a) and 3(b), the polyspline used may cause additional broadening. Using a fitting procedure Tan *et al.* determine the first neighbor Co-Si distance for their sample as 2.32 ± 0.02 Å. The implantation dose of 1.0×10^{17} Co atoms/cm^2 was slightly lower than for our 1.4×10^{17} Co atoms/cm^2 sample and though other preparation conditions may differ as well, the agreement with the distance of 2.32 ± 0.05 Å determined for our IBS sample is striking. We attribute the slightly larger error in our analysis to uncertainties in the shape of the background due to the influence of the Co L_1 near edge structure and the shorter wave vector range covered.

The same L EXAFS technique as outlined above for Co should in principle be applicable to silicides formed by other 3d TM's. Problems due to the superposition of the EXAFS oscillations due to L_3 and L_2 absorption channels are lower for the earlier 3d TM's due to the smaller spin-orbit splitting. On the other hand, the L_1 edge is closer to the $L_{2,3}$ absorption thresholds for the earlier 3d TM's. Consequently, regions II and III, shown in Fig. 1, which are influenced by modeling the L_1 near edge structure, are extended at the expense of region I. This is likely to increase the error of the L EXAFS analysis for early 3d TM's due to imperfections in the modeled background. Of course, the opposite is true for late 3d TM's: Region I, unaffected by L_1 modeling imperfections, is extended.

In order to investigate early 3d TM's, to improve the accuracy for the determination of the first shell distance, and to determine distances to the second and higher shells, it is therefore necessary to minimize the number of free parameters used to simulate the backgound due to the L_1 absorption. Thus it would be most favorable if the shape of the L_1 absorption could be determined by an experiment.

The superposition of the $L_{2,3}$ EXAFS features is obviously a problem for such a measurement. Temperature dependent measurements could be used to separate the EXAFS from the L_1 near edge structure since the EXAFS amplitudes should be reduced with higher temperatures. However, the TM L_1 absorption could be selectively monitored if a process specifically related to the decay of a TM 2s core hole is chosen. For buried samples this could be achieved by partially measuring the TM L_γ fluorescence radiation, generated by the radiative decay of the 2s core vacancy. Since this radiation has to be separated from the much stronger TM L_α and L_β emission generated by the decay of the 2p core holes, this requires fluorescence detectors with an energy resolution better than 50 eV at 900 eV photon energy. Alternatively, the information concerning the L_1 absorption could be extracted from a nonburied sample by partially monitoring the Auger decay of the TM 2s core vacancy.

Keeping these future refinements in mind, we believe that L EXAFS is a promising alternative for the study of 3d TM compounds in crystalline environments.

An additional advantage of L EXAFS for 3d TM compounds is the fact that the electronic structure can be studied parallel to the geometric structure by investigating the 3d TM $L_{2,3}$ near edge structure. This near edge region contains information about the unoccupied electronic states of d symmetry in the TM. These d states dominate the valence electronic structure in 3d TM silicides and are therefore important for the bonding in these compounds.[22,15].

IV. CONCLUSION

L EXAFS of 3d TM's as a method of studying the geometric structure of 3d TM silicides buried in a Si wafer has been presented. In contrast to K EXAFS for these systems, this technique is easily compatible with the FY detection mode needed to investigate the buried structures *in situ*. The main problem for the data analysis in L EXAFS is the superposition of the L_1 absorption features to the $L_{2,3}$ EXAFS oscillations. This problem can be overcome by accounting for this additional background by a polysplining procedure. The technique has been demonstrated for a buried $CoSi_2$ sample produced by IBS, where the first neighbor Co-Si distance has been determined as 2.32 ± 0.05 Å, in good agreement with the $CoSi_2$ literature value of 2.323 Å.

ACKNOWLEDGMENTS

We are grateful to R. Jebasinski and S. Mantl for kindly providing the IBS $CoSi_2$ samples. We would like to thank S. Cramm and U. Döbler for valuable discussions and K. Holldack for his help at the HE-PGM2 at BESSY.

[1] J.C. Hensel, A.F. Levi, R.T. Tung, and J.M. Gibson, Appl. Phys. Lett. **47**, 151 (1985).

[2] A. Schüppen, S. Mantl, L. Vescan, and H. Lüth, in *Proceedings of the European Solid State Device Research Conference–90, Nottingham*, edited by W. Eccleston and P.J. Rosser (Institute of Physics and Physical Society, London, 1990), p. 45.

[3] S.P. Murarka, in *Silicides for VLSI Applications* (Academic, New York, 1983).

[4] S. P. Murarka and M.C. Peckerar in *Electronic Materials, Science and Technology* (Academic, Boston, 1989), p. 267.

[5] S. Mantl, Mater. Sci. Rep. **8**, 1 (1992).

[6] J. Jaklevic, J.A. Kirby, M.P. Klein, A.S. Robertson, G.S. Brown, and P. Eisenberger, Solid State Commun. **23**, 679 (1977).

[7] S. Eisebitt, T. Böske, J.-E. Rubensson, and W. Eberhardt, Phys. Rev. B **47**, 14 103 (1993).

[8] L. Tröger, D. Arvanitis, K. Baberschke, H. Michaelis, U. Grimm, and E. Zschech, Phys. Rev. B **46**, 3283 (1992).

[9] Z. Tan, F. Namavar, J.I. Budnick, F.H. Sanchez, A. Fasi-

huddin, S.M. Heald, C.E. Bouldin, and J.C. Woicik, Phys. Rev. B **46**, 4077 (1992).
[10]D. Denley, R.S. Williams, P. Perfetti, D.A. Shirley, and J. Stöhr, Phys. Rev. B **19**, 1762 (1979).
[11]H. Meyerheim, Ph.D. thesis, Freie Universität Berlin, 1990.
[12]R. Jebasinski, S. Mantl, L. Vescan, and Ch. Dieker, Appl. Surf. Sci. **53**, 264 (1991).
[13]*Pearson's Handbook of Crystallographic Data for Intermetallic Phases, Vol. 1,* edited by P. Villars and L.D. Calvert (American Society for Metals, Metals Park, OH, 1985).
[14]D. Bahr, W. Press, R. Jebasinski, and S. Mantl, Phys. Rev. B **47**, 4385 (1993).
[15]S. Eisebitt, T. Böske, J.-E. Rubensson, R. Jebasinski, S. Mantl, J. Kojnok, P. Skytt, J.-H. Guo, N. Wassdahl, J. Nordgren, K. Holldack, and W. Eberhardt, Phys. Rev. B **48**, 5042 (1993).
[16]H. Petersen, Nucl. Instrum. Methods Phys. Res. A **246**, 260 (1986).
[17]J. C. Fuggle and N. Mårtensson, J. Electron Spectrosc. **21**, 275 (1980).
[18]J.J. Yeh and I. Lindau, At. Data Nucl. Data Tables **32**, 47 (1985).
[19]W.J. Veigele, in *Handbook of Spectroscopy*, edited by J.W. Robinson (CRC Press, Cleveland, 1974), Vol. 1.
[20]B. Lengeler and P. Eisenberger, Phys. Rev. B **21**, 4507 (1980).
[21]Z. Tan, J.I. Budnick, F.H. Sanchez, G. Tourillon, F. Namavar, and H.C. Hayden, Phys. Rev. B **40**, 6368 (1989).
[22]G.W. Rubloff, Surf. Sci. **132**, 268 (1983).